A Physics-Based Approach to Simulate Jet Engines

Sami S. Mina
Rockwell Collins Simulation and Training Solutions
Sterling, VA
sami.mina@rockwellcollins.com

ABSTRACT

Creating jet engine simulations that replicate the behavior of actual engine parameters at finite flight conditions is only one step toward meeting the requirements for pilot training. Reproducing realistic performance trends throughout the flight envelope and generating proper responses to malfunctions and pilot-initiated events, including secondary and cascading effects, is critical to achieving positive pilot training.

Traditionally, jet engine simulation for pilot training purposes is based on table-lookup of steady-state engine parameters, such as rotor rotational speed, fuel flow, exhaust gas temperature, engine pressure ratio and net thrust. This approach does not inherently meet all the aforementioned requirements and exhibits the following shortcomings: The dynamic engine performance has to be approximated as a lagged transition between steady-state points. It is unreliable to predict the behavior of the engine parameters when excursions outside the bounds of the tables take place. Malfunction effects have to be programmed individually for each engine parameter and for different flight and operational conditions. Additionally, the interdependencies between the different engine parameters can be violated during the model tuning process. Accordingly, a new approach to model jet engines is needed.

The objective of this paper is to present a physics-based jet engine simulation approach which addresses the shortcomings of table-lookup solutions, is data-driven and generic, while also distinguishing itself from other physics-based simulations (Claus, Townsend, 2010) by being computationally efficient. This approach can be used to simulate any turbojet or turbofan engine by accounting for the physical processes and the geometric and mechanical characteristics that govern the performance and behavior of the engine. These include the fan, compressors and turbines maps, the rotors inertia, and the thermodynamics of the flow entering the engine from its free-stream state ahead of the engine intake, through the intake duct, the fan, the compressors, the combustion chamber, the turbines and the nozzles.

The paper discusses the methodology used in applying the physics-based approach to simulate a two-spool turbofan engine, the technical challenges involved and demonstrates how this new approach advantageously compares with a table-lookup model in matching actual flight test data and in providing realistic performance trends.
The paper also assesses the physics-based approach's ability to meet the requirements of the different levels of flight simulators and flight training devices, as defined in FAR 14 CFR Part 60.

ABOUT THE AUTHOR

Sami S. Mina is a Principal Systems Engineer in the Vehicle Dynamics group at Rockwell Collins Simulation and Training Solutions (RC-STS) in Sterling, VA. His position entails defining and generating high-fidelity real-time architectures and models to simulate aircraft performance and handling characteristics, as well as modeling the flight environment. Sami has 39 years experience in the aerospace engineering field. These cover aircraft operations, airframe and engine performance monitoring and flight path optimization, advanced aircraft design, flight testing, and flight simulation. He has been at RC-STS for over 16 years during which he has conducted flight testing and worked on a large number of simulators with many certified to FAR 14 CFR Part 60 level D. Recently, he has developed advanced solutions for the equations of motion of flight vehicles, high fidelity ground reaction models, and data-driven automatic fidelity testing environment. Sami holds a Bachelors Degree in Aeronautical Engineering (1975) and a Masters Degree in Aeronautical Engineering (1979), both from Cairo University. He is a senior member of the American Institute of Aeronautics and Astronautics and the Canadian Aeronautics and Space Institute.

A Physics-Based Approach to Simulate Jet Engines

Sami S. Mina
Rockwell Collins Simulation and Training Solutions
Sterling, VA
sami.mina@rockwellcollins.com

BACKGROUND

The simulation of jet engines is a complex task that involves replicating the behavior of numerous engine performance parameters under varying environmental and operational conditions.

Table 1 shows the main performance parameters for a typical two-spool turbofan engine. (See Appendix A. Glossary for the corresponding acronyms, abbreviations and symbols used throughout this paper.)
In table-lookup simulations, the tables provide the steady-state values which are usually generated from a stand-alone application provided by the engine manufacturer and known as an "Engine Deck". The transient states are derived in real-time from the steady states using lag functions. Additionally, the gross thrust, ram drag and mass flows are frequently not provided and only net thrust may be available. This could affect the simulation versatility and limit its applicability to certain aircraft classes. To circumvent these limitations an estimation of the mass flows is needed in order to derive the ram drag and combined with the net thrust the gross thrust can then be generated. This decomposition of the net thrust into gross thrust and ram drag extends the simulation's fidelity into high angle of attack flight regimes where the gross thrust and the ram drag are highly misaligned. Additional performance parameters, such as the pressures and temperatures at different engine stations, may be needed by bleeds used for deicing and cabin pressurization and heating or for feedback into engine controllers and monitoring systems. However, these parameters are typically absent in table-lookup models.

Table 1. Performance Parameters

Gross Thrust
Net Thrust
Ram Drag
Engine Pressure Ratio
Low Pressure Spool Rotational Velocity
High Pressure Spool Rotational Velocity
Fuel Flow
Exhaust Gas Temperature
Inter-Turbine Temperature
Primary/Core Mass Flow
Secondary/Bypass Mass Flow

Table 2 shows the main environmental parameters affecting the performance of jet engines. In table-lookup solutions, these would be the input variables and along with the operational parameters will dictate the tables' dimensions. Typically, pressure altitude, Mach number and ambient temperature are used in the performance parameters' main tables' lookup, whereas the effect of additional miscellaneous parameters, such as relative air humidity, are either treated as increments or even entirely ignored.

Table 2. Environmental Parameters

Pressure Altitude
Mach Number
Ambient Temperature
Inlet Flow Distortion
Water and Ice Ingestion
Relative Air Humidity

Table 3 shows the main operational parameters affecting the performance of jet engines. In table-lookup solutions the throttle position is either used directly as the input lookup variable or is fed into an engine controller which commands the fuel flow used for the lookup. The effects of the other parameters in table 3 are either partly ignored, treated as crude increments or dictate the use of additional and interchangeable full sets of tables in order to avoid having main tables with too many dimensions. A scheme is then devised to switch and transition between the table sets.

Table 3. Operational Parameters

Throttle Position
Bleeds
Power Extraction
Inlet Guide Vanes Position
Intake Pressure Relief Doors Position
Nozzle Position
Thrust Reverser Position
Ignition Status
Starter Torque
Damage and Malfunctions
Fuel Calorific Value

PHYSICS-BASED MODEL

It has become clear from the discussion above that a table-lookup solution requires extensive knowledge of the behavior of each engine performance parameter across the entire flight envelope and under all operational conditions. For example, the table-lookup approach requires specific flight test data on compressor deterioration to answer questions such as: By how much would the thrust decrease if the compressor efficiency dropped by 5% due to blade erosion? And would that lead to a decrease or an increase in rotational speed, and by how much? And what about the fuel flow or the exhaust gas temperature? This contrasts with the physics-based solution which inherently provides the proper trends and relative deviations among all the engine performance parameters. Furthermore, with just a few flight data points the physics-based model can be tuned to also provide a reasonably accurate answer. As will be explained below, the physics-based approach is an engine model. Specifically, it models the engine components unlike strictly mathematical solutions, such as those based on regression analysis of inputs and outputs, or those that account for environmental and operational effects through the use of mathematical expressions involving partial derivatives and described in the comprehensive survey by Sanghi, Lakshmanan, Sundararajan (2000).

Figure 1 shows the top-level architecture of the physics-based engine model. The main inputs to the model are the fuel flow and the environmental conditions: Mach number, ambient pressure and ambient temperature, along with the nozzles geometry and spools inertia. A thermodynamic cycle analysis (see Appendices B and C) is used to compute the pressure and temperature at each engine station (see Figure 2), as well as the mass flows, gross thrust, ram drag and the net power for each spool. Figure 1 also shows the progression from spool power to torque, to spool acceleration by using the current rotational speed and spool inertia, respectively. The spool's rotational speed is then updated by integrating its acceleration. The rotational speeds, along with the mass flows are subsequently fed into the fan, compressors and turbines maps in order to calculate their pressure ratios, which are in turn fed back into the thermodynamic cycle.

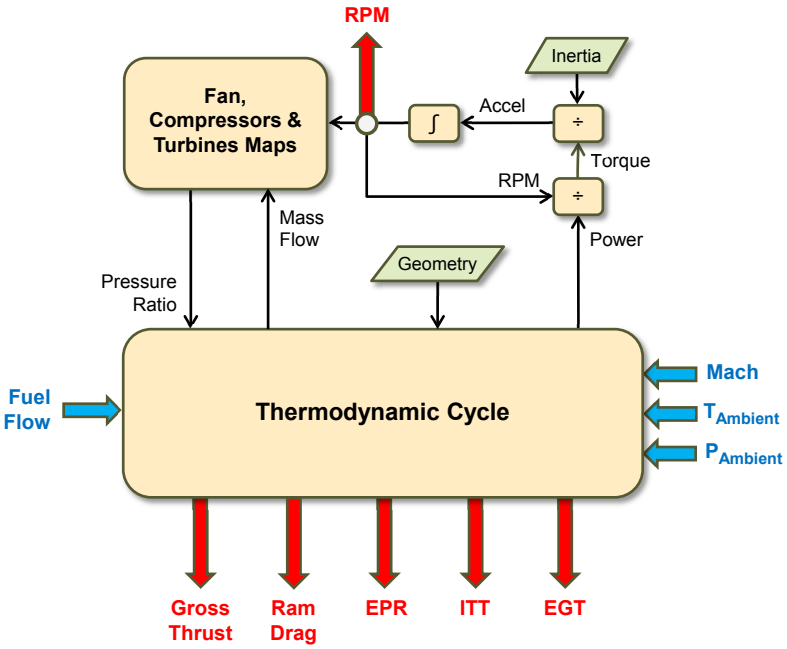

Figure 1. Physics-Based Model Architecture

The model handles any number of spools. Thus it can simulate a ramjet with no spools, a single-spool turbojet or a two-spool or three-spool turbofan. The model also handles geared-fan engine configurations.

Figure 2 introduces a two-spool turbofan engine's stations and their notation as used throughout this paper. Station 0 represents the free undisturbed airflow at ambient conditions. Stations 1 through 8 represent the entries into the intake, fan, low pressure compressor, high pressure compressor, combustion chamber, high pressure turbine, low pressure turbine, and primary or core nozzle, respectively. Station 3 also represents the entry into the secondary or bypass nozzle, while stations 9 and 10 represent the core and bypass nozzles' exits, respectively.

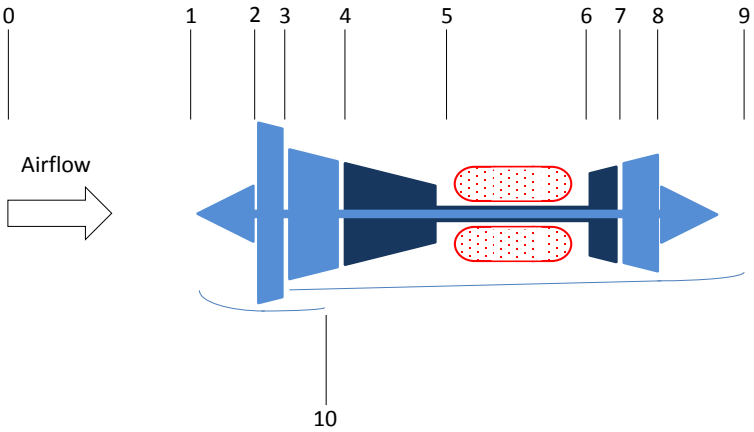

Figure 2. Two-Spool Turbofan Engine Stations

Typically, the airflow entering the intake goes through the fan before being split into two parts. The core flow which continues through the low pressure compressor and the rest of the engine, and the bypass flow which exits through the bypass nozzle. The mass flow in the combustion chamber and all components downstream of it also includes the fuel flow, besides the core flow. This characterization of the engine's mass flow breakdown is too simplistic. Actual engines have bleeds at different compressor stages to meet the demands of cabin heating and pressurization, aircraft surface deicing, pneumatic system, and compressor stall protection. These are accounted for in this physics-based model by breaking down a compressor into smaller virtual compressors along each bleed valve location, with each virtual compressor having a different mass flow but all still sharing the same shaft and thus having the same rotational speed and all contributing to the power load on that shaft.

Assumptions

Component efficiencies and loss factors were estimated based on the simulated engine's vintage and design features for the following parameters: Intake pressure recovery, fan, low pressure and high pressure compressors thermodynamic efficiencies, combustion efficiency, combustion chamber total pressure loss, low and high pressure turbines polytropic efficiencies and spools' mechanical efficiencies. To simulate a degraded or damaged component its corresponding efficiency is decreased or its associated loss factor is increased. The thermodynamic process for each engine component used values, for the specific heat at constant pressure (c_p) and the specific heat ratio (γ) for air or combustion gas, based on the average total temperature across that component and on the flow composition.

Fan and Compressors Maps

No attempt was made to generate the fan and compressors maps in real-time. Instead, the fan, low pressure compressor and high pressure compressor maps were generated using an offline application based on the work of MacIsaac, Langton (2011). Figure 3 shows the generated map of a high pressure compressor. This approach extends the map well past the compressor stall and into the chocked regime where both the airflow and the pressure ratio drop. A surge line is added based on an estimate of the maximum allowable compressor stage loading.

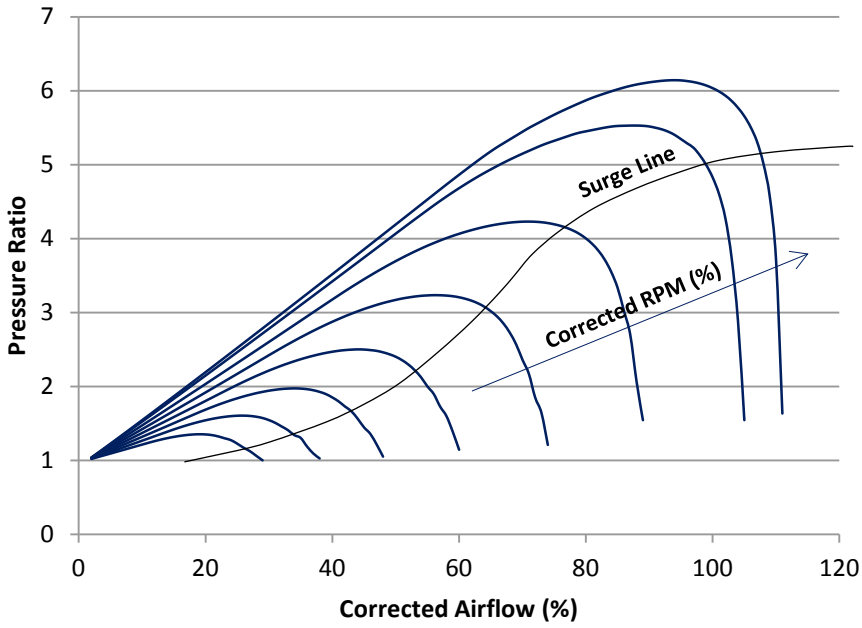

Figure 3. Compressor Map

Turbine Maps and Component-Matching

The low and high pressure turbine maps were also generated using an offline tool. However, these could not be generated solely based on the turbines known geometric characteristics, as they needed to be matched to the fan and compressors with whom they share a shaft. This component-matching problem is not unlike the one an engine designer must face: For given environmental and operational conditions the fan and the compressor, which are power consumers, and the turbine, a power generator, must find a common shaft rotational speed at which they are in a stable equilibrium. Furthermore, progressively increasing the fuel flow should result in a progressively increasing rotational velocity, from idle to maximum power setting. The engine should neither flame-out nor accelerate to self-destruction. This was achieved by solving for the turbine power, and consequently the turbine total temperature ratio, that is needed to equate the fan or compressor power when both are at the same rotational velocity (see Appendix D). The required turbine total pressure ratio is then derived from the total temperature ratio. The two-spool configuration proved particularly challenging as any map adjustments to match the components on one spool affected the equilibrium of the other spool, necessitating an iterative matching approach.

Steady-State Performance Tuning

The component-matching process described above was repeated at several points across the flight envelope with minor adjustments to the components' maps and efficiencies in order to replicate the steady-state engine performance.

Transient Performance Tuning

Initial estimates of the spools' inertia were made based on their geometry and material. These were later refined in order to match the engine dynamic response.

Table 4 and Figure 4 show the PBM engine dynamic response to a throttle slam during a go-around maneuver along with the actual engine criteria. This engine acceleration test is required for FAA certification of FFS according to FAR 14 CFR Part 60.

The PBM demonstrates a good match of the flight test data and the acceleration times *Ti* and *Tt* (defined below) are shown to meet the FAA requirements for Level D FFS.

Ti—Total time from initial throttle movement until a 10% response of a critical engine parameter.

Tt—Total time from initial throttle movement to an increase of 90% of go around power.

A traditional table-lookup model, using lag functions to transition between steady-state data points, would also be tuned to meet the requirements of this test by adjusting its lag function parameters. However, when real-life arbitrary throttle handling is performed, the table-lookup model's response (Figure 5 in pink) is unrealistic since the lag function parameters were optimized for a full throttle slam and are wholly inadequate to handle incremental throttle movements including reversals. Figure 5 also demonstrates the physics-based model's far more compliant behavior (in green).

Table 4. Engine Acceleration Times Analysis

Parameter	Tolerance	Aircraft	PBM	Grade
Ti (sec)	0.25	1.308	1.370	Pass
Tt (sec)	10%	5.116	4.841	Pass

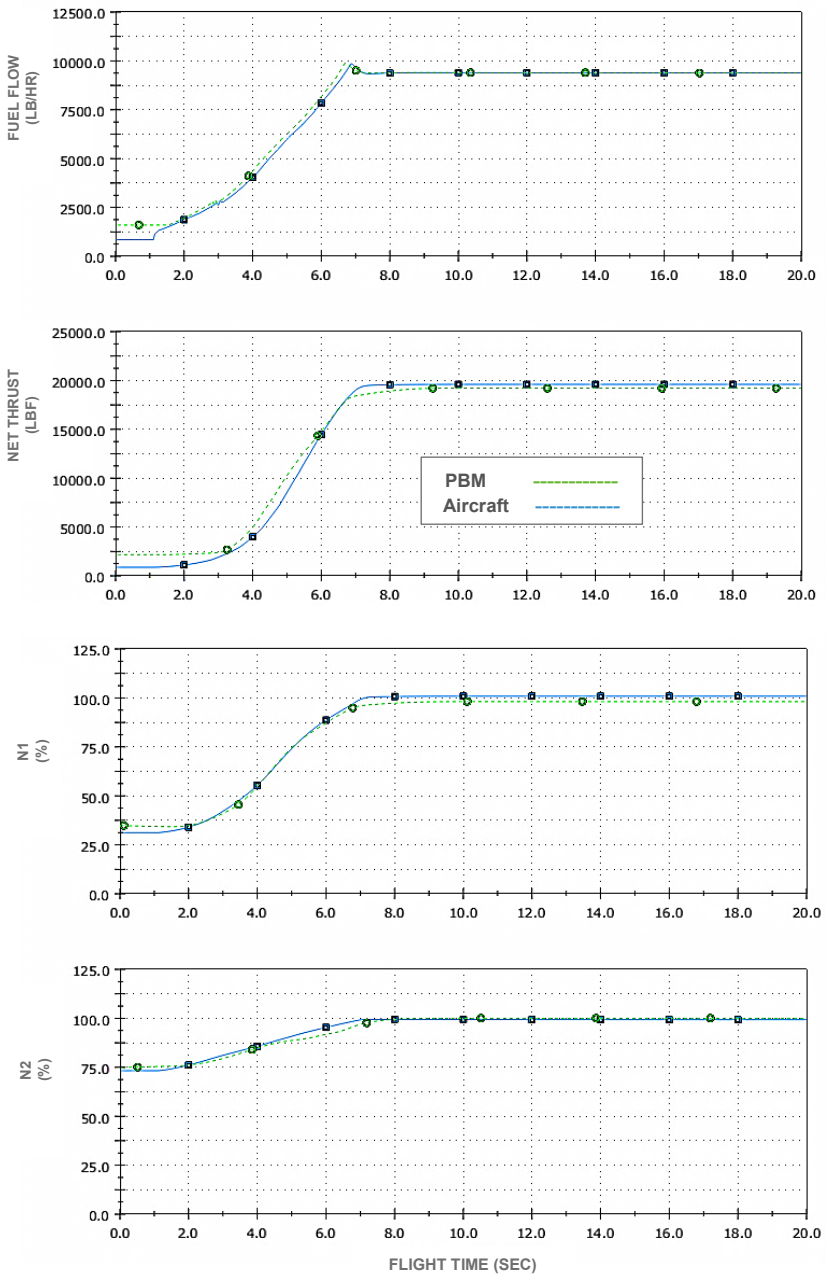

Figure 4. Engine Acceleration

Engine Sizing

An examination of the thermodynamic cycle analysis in Appendix C shows that all the thermodynamic formulation, from the free-stream air all the way to the core and bypass flow nozzle entries, deals with pressures and temperatures and makes no reference to the engine size, mass flow, gross thrust or ram drag. These size-dependent parameters are only dealt with starting with the derivation of the mass flows in the nozzles analyses. This reveals the inherent ability of the physics-based approach to scale the solution and generate families of engine models by changing the nozzles' dimensions. The only other size-dependent parameters are the spools' inertia and these will need to be adjusted to get the proper acceleration response of the newly-sized engine.

Computational Requirements

When tested in a full real-time simulation running at a 60Hz rate on a server with a quad Intel(R) Xeon(R) E5240 processor running @ 3.00GHz (PassMark(R) CPU Mark of 2492), the average processing time of the Physics-Based Model was 65µsec compared to a table-lookup model time of 28µsec. These times represent about 0.39% and 0.17% of the simulation frame time, respectively. Despite the fact that the PBM model more than doubled the engine simulation computational requirements compared to a table-lookup model, both demonstrated a very low computational load and both remain viable real-time solutions.

Model Fidelity

When the development of the PBM started, the expectations were that it would most certainly meet the requirements of lower fidelity FTD devices. The question was whether it would meet those of the higher fidelity FFS simulators. Paradoxically, it was demonstrated that the PBM was more suited for the higher level FFS simulators because of its inherent realistic trends and correct parameters' interrelationships. Conversely, the fact that it required careful turbine/compressor matching may make it less attractive to the developer of lower level FTD devices who would rather enjoy the freedom, afforded by the table-lookup model, to always provide any desired output without regard to its quality or trend.

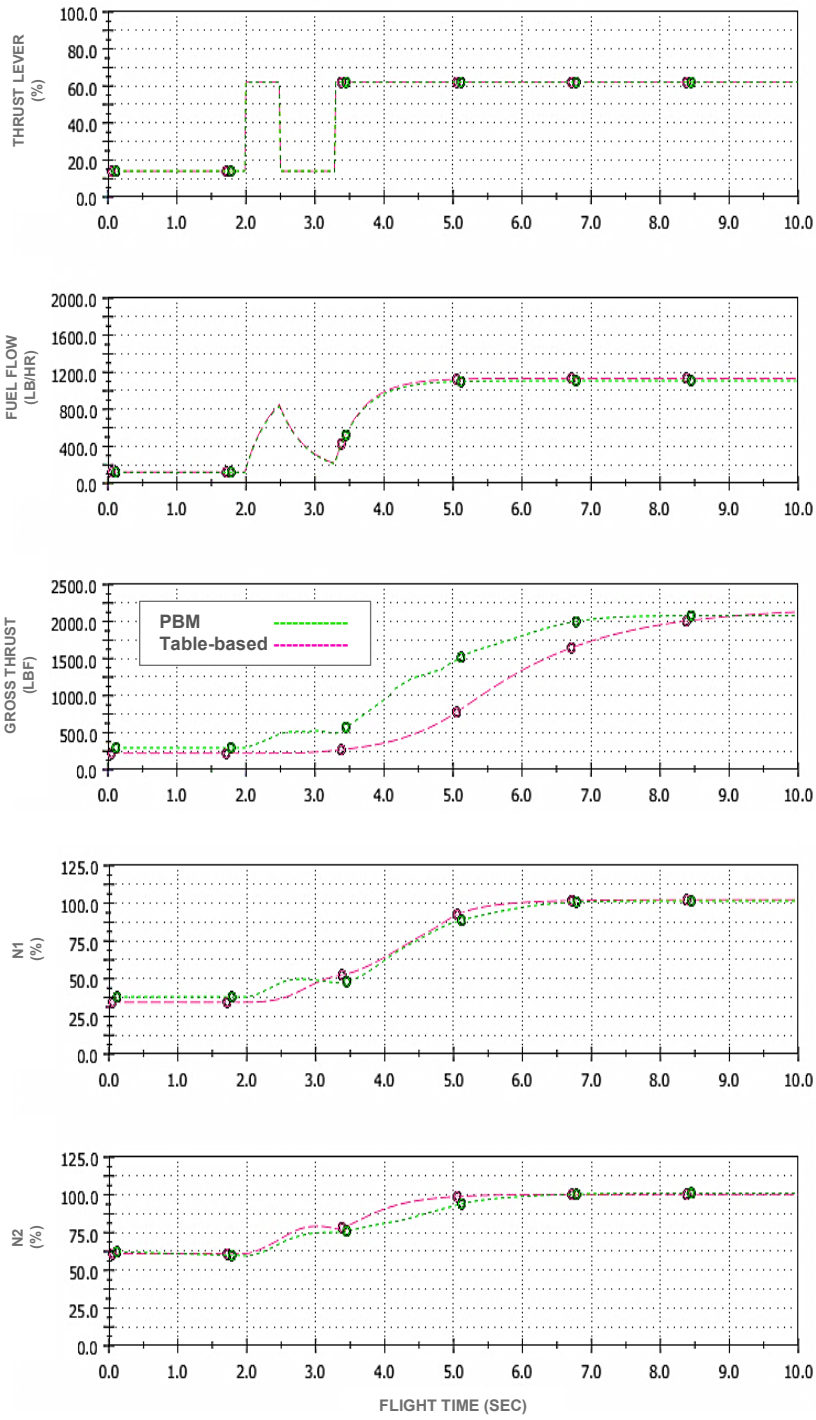

Figure 5. Engine Response to Arbitrary Throttle Input

CONCLUSION

A physics-based jet engine model was developed and compared to a traditional table-lookup model. The physics-based model was assessed against the FTD and FFS certification requirements of FAR 14 CFR Part 60. It was demonstrated that the physics-based jet engine model approach is a viable option for the purpose of real-time pilot training. It is inherently capable of a higher level of fidelity as compared to a table-lookup model. It ensures realistic engine performance trends across the flight envelope and under real-life pilot throttle input as opposed to replicating only the test cases collected or chosen for the purpose of simulator certification. It was also shown that its computational requirements, though higher that those of the table-lookup approach, remain fairly modest through the use of offline generation of the fan, compressors and turbines maps. These conclusions need to be further substantiated by full development, certification and deployment of a training device incorporating this model. Additionally, the learning curve for developing an engine model and tuning it to match flight test data using this physics-based approach, by someone other than the author, has not been investigated.

APPENDIX A - Glossary

Acronyms & Abbreviations

EGT	exhaust gas temperature
EPR	engine pressure ratio
FAA	federal aviation administration
FAR	federal air regulations
FF	fuel flow
FFS	full flight simulator
FTD	flight training device
ITT	inter-turbine temperature
PBM	physics-based model presented in this paper
RPM	revolution per minute

Symbols

A	nozzle exit area
c_p	specific heat at constant pressure
f	fuel to air ratio
F	force
h	fuel calorific value
$\dot{m}$	mass flow
M	flow Mach number (with subscript) or flight Mach number (no subscript)
P	pressure
Q	heat energy rate
R	universal gas constant
T	temperature
v	flow velocity (with subscript) or true airspeed (no subscript)
β	bypass ratio
γ	specific heat ratio
η	efficiency
π	pressure ratio or pressure recovery factor
ρ	density

Subscripts

a	air
$bypass$	bypass flow
ch	high pressure compressor
cl	low pressure compressor
com	combustion
$core$	core flow
$crit$	critical – corresponds to a choked nozzle

D	drag
f	fan
full	full – corresponds to ambient pressure at nozzle exit
g	gas
G	gross
hp	high pressure spool
i	intake
lp	low pressure spool
m	mechanical
n	nozzle
o	ambient
p	polytropic
t	total
th	high pressure turbine
tl	low pressure turbine
1, 2, 3 …	engine station

Superscripts

′	isentropic

APPENDIX B - The T-s Diagram

Figure 6 shows the Temperature-Entropy (T-s) diagram for a Brayton cycle. The engine station notation shown is that for the two-spool turbofan engine described in Figure 2. Q is the heat energy added per unit of core mass flow per time unit. For all stations the total conditions are shown except for stations 0, 9 and 10 where the static conditions are shown instead. Station 1 is not shown since the flow may accelerate or decelerate ahead of the intake in an isentropic process. Thus both stations 0 and 1 will have the same total conditions. No isentropic processes are assumed to take place within the engine: All flow compression in the intake, fan and compressors and flow expansion in the turbines and nozzles increase the entropy.

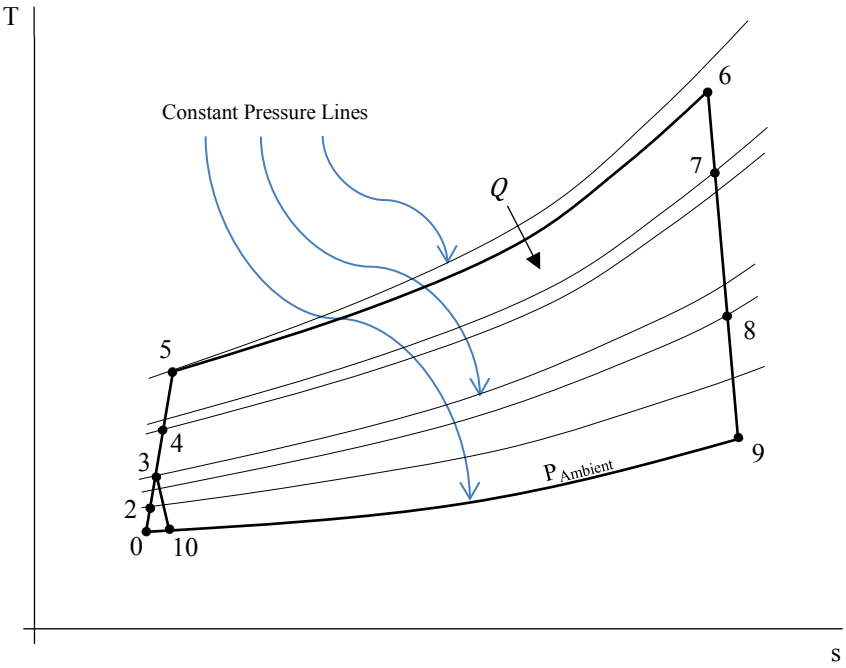

Figure 6. T-s Diagram

Ignoring shaft power extraction and bleeds, the difference in total temperatures between stations 4 and 5 is very close to that between stations 6 and 7. This is because, for steady-state conditions, the high pressure turbine power equals that of the high pressure compressor. The small total temperature difference mismatch is due to the difference in the specific heat at constant pressure (c_p) between the turbine hot combustion gas flow and the cooler compressor airflow and the additional fuel flow going through the turbine. Similarly, the low pressure turbine power equals that of the low pressure compressor and the fan combined. However, the difference in total temperature between stations 2 and 4 is vastly smaller than that between stations 7 and 8 since both the bypass and core flows go through the fan but the turbine flow, aside from including the fuel flow, is mostly made up of the core flow only. The static conditions shown at the nozzles' exits (stations 9 and 10) assume full flow expansion to ambient pressure.

APPENDIX C - Thermodynamic Cycle Analysis

Intake

$$P_{t1} = P_{to} = P_o(1 + \frac{\gamma - 1}{2} M^2)^{\frac{\gamma}{\gamma-1}} \quad (1)$$

$$P_{t2} = P_{t1}\,\pi_i \quad (2)$$

$$T_{t2} = T_{t1} = T_{to} = T_o(1 + \frac{\gamma - 1}{2} M^2) \quad (3)$$

Fan

$$P_{t3} = P_{t2}\,\pi_f \quad (4)$$

$$T'_{t3} = T_{t2}\,\pi_f{}^{\frac{\gamma-1}{\gamma}} \quad (5)$$

$$T_{t3} = \frac{1}{\eta_f}(T'_{t3} - T_{t2}) + T_{t2} \quad (6)$$

Low Pressure Compressor

$$P_{t4} = P_{t3}\,\pi_{cl} \quad (7)$$

$$T'_{t4} = T_{t3}\,\pi_{cl}{}^{\frac{\gamma-1}{\gamma}} \quad (8)$$

$$T_{t4} = \frac{1}{\eta_{cl}}(T'_{t4} - T_{t3}) + T_{t3} \quad (9)$$

High Pressure Compressor

$$P_{t5} = P_{t4}\,\pi_{ch} \quad (10)$$

$$T'_{t5} = T_{t4}\,\pi_{ch}{}^{\frac{\gamma-1}{\gamma}} \quad (11)$$

$$T_{t5} = \frac{1}{\eta_{ch}}(T'_{t5} - T_{t4}) + T_{t4} \quad (12)$$

Combustion Chamber

$$P_{t6} = P_{t5}\,\pi_{com} \quad (13)$$

$$Q = FF\ \ h\ \ \eta_{com} \quad (14)$$

$$T_{t6} = T_{t5} + \frac{Q}{\dot{m}\ \ c_p} \quad (15)$$

High Pressure Turbine

$$P_{t7} = P_{t6}\,\pi_{th} \quad (16)$$

$$T'_{t7} = T_{t6}\,\pi_{th}{}^{\frac{\gamma-1}{\gamma}} \quad (17)$$

$$T_{t7} = \eta_{th}(T'_{t7} - T_{t6}) + T_{t6} \quad (18)$$

Low Pressure Turbine

$$P_{t8} = P_{t7}\,\pi_{tl} \quad (19)$$

$$T'_{t8} = T_{t7}\,\pi_{tl}{}^{\frac{\gamma-1}{\gamma}} \quad (20)$$

$$T_{t8} = \eta_{tl}(T'_{t8} - T_{t7}) + T_{t7} \quad (21)$$

Core Nozzle

$$P_{t9} = P_{t8}\,\pi_{n_{core}} \quad (22)$$

$$T_{t9} = T_{t8} \quad (23)$$

for chocked convergent nozzle

$$\pi_{crit_{core}} = \frac{2}{\gamma + 1}^{\frac{\gamma}{\gamma-1}} \quad (24)$$

$$P_9 = P_{t9}\,\pi_{crit_{core}} \quad (25)$$

$$T_9 = T_{t9}\,\frac{2}{\gamma + 1} \quad (26)$$

$$M_9 = 1 \quad (27)$$

for full flow expansion

$$\pi_{full_{core}} = \frac{P_o}{P_{t9}} \tag{28}$$

$$P_9 = P_o \tag{29}$$

$$T_9 = T_{t9}\, \pi_{full_{core}}{}^{\frac{\gamma-1}{\gamma}} \tag{30}$$

$$M_9 = \sqrt{\left[\left(\frac{1}{\pi_{full_{core}}}\right)^{\frac{\gamma-1}{\gamma}} - 1\right]\frac{2}{\gamma-1}} \tag{31}$$

$$v_9 = M_9\sqrt{\gamma\, R\, T_9} \tag{32}$$

$$\rho_9 = \frac{P_9}{R\, T_9} \tag{33}$$

$$\dot{m}_9 = \rho_9\, v_9\, A_9 \tag{34}$$

Bypass Nozzle

$$P_{t10} = P_{t3}\, \pi_{n_{bypass}} \tag{35}$$

$$T_{t10} = T_{t3} \tag{36}$$

for chocked convergent nozzle

$$\pi_{crit_{bypass}} = \frac{2}{\gamma+1}^{\frac{\gamma}{\gamma-1}} \tag{37}$$

$$P_{10} = P_{t10}\, \pi_{crit_{bypass}} \tag{38}$$

$$T_{10} = T_{t10}\, \frac{2}{\gamma+1} \tag{39}$$

$$M_{10} = 1 \tag{40}$$

for full flow expansion

$$\pi_{full_{bypass}} = \frac{P_o}{P_{t10}} \tag{41}$$

$$P_{10} = P_o \tag{42}$$

$$T_{10} = T_{t10}\, \pi_{full_{bypass}}{}^{\frac{\gamma-1}{\gamma}} \tag{43}$$

$$M_{10} = \sqrt{\left[\left(\frac{1}{\pi_{full_{bypass}}}\right)^{\frac{\gamma-1}{\gamma}} - 1\right]\frac{2}{\gamma-1}} \tag{44}$$

$$v_{10} = M_{10}\sqrt{\gamma\, R\, T_{10}} \tag{45}$$

$$\rho_{10} = \frac{P_{10}}{R\, T_{10}} \tag{46}$$

$$\dot{m}_{10} = \rho_{10}\, v_{10}\, A_{10} \tag{47}$$

Gross Thrust

$$\dot{m}_{core} = \dot{m}_9 - FF \tag{48}$$

$$\dot{m}_{bypass} = \dot{m}_{10} \tag{49}$$

$$F_G = (\dot{m}_{core} + FF)v_9 + \dot{m}_{bypass}\, v_{10} + A_{core}\,(P_9 - P_o) + A_{bypass}\,(P_{10} - P_o) \tag{50}$$

Ram Drag

$$F_D = \left(\dot{m}_{core} + \dot{m}_{bypass}\right) v \tag{51}$$

APPENDIX D – Compressor / Turbine Power Matching

High Pressure Spool

$$T_{t7} = T_{t6} - \frac{c_{p_{a_{ch}}}}{c_{p_{g_{th}}}} \frac{(T_{t5} - T_{t4})}{\eta_{m_{hp}} (1+f)} \tag{52}$$

$$T'_{t7} = T_{t6} - \frac{1}{\eta_{th}} (T_{t6} - T_{t7}) \tag{53}$$

$$\pi_{th} = \left(\frac{T'_{t7}}{T_{t6}}\right)^{\frac{\gamma}{\gamma-1}} \tag{54}$$

Low Pressure Spool

$$T_{t8} = T_{t7} - \frac{c_{p_{a_f}} (1+\beta) (T_{t3} - T_{t2}) + c_{p_{a_{cl}}} (T_{t4} - T_{t3})}{c_{p_{g_{tl}}} \eta_{m_{lp}} (1+f)} \tag{55}$$

$$T'_{t8} = T_{t7} - \frac{1}{\eta_{tl}} (T_{t7} - T_{t8}) \tag{56}$$

$$\pi_{tl} = \left(\frac{T'_{t8}}{T_{t7}}\right)^{\frac{\gamma}{\gamma-1}} \tag{57}$$

ACKNOWLEDGEMENTS

I would like to thank Mr. Nick Giannias, Senior Technical Fellow at CAE and a member of the Simulation Subcommittee for I/ITSEC 2014, for the guidance and insight he provided me during the writing of this paper and for his many comments and critical reviews of the paper's drafts.
I would also like to thank Mr. Harold T. Peeling, Principal Software Engineer at Rockwell Collins, for generating the fan and compressors maps. His contribution was invaluable and helped the presented physics-based model achieve a level of fidelity higher than what I expected at the outset of this work.

REFERENCES

Claus, R. W., Townsend, S. (2010). A Review of High Fidelity, Gas Turbine Engine Simulations. 27th *International Congress of the Aeronautical Sciences Proceedings.*

MacIsaac, B., Langton, R., (2011). *Gas Turbine Propulsion Systems - Appendix B Estimation of Compressor Maps.* John Wiley & Sons, Ltd.

Sanghi, V., Lakshmanan, B. K. & Sundararajan, V. (2000). Survey of Advancements in Jet-Engine Thermodynamic Simulation. *Journal of Propulsion and Power, Vol. 16, No. 5.*